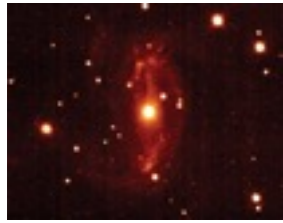


**NuSTAR spectral analysis of the two
bright Seyfert 1 galaxies:
MCG 8-11-11 and NGC 6814**

Overview

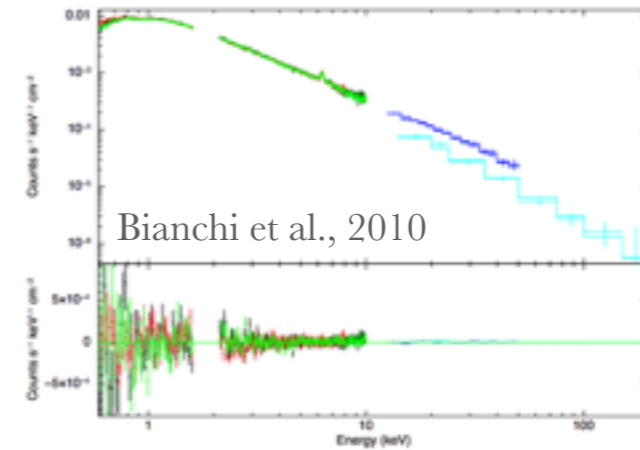


MCG +8-11-11

$$z = 0.0204$$

$$F_{2-10\text{keV}} = 5.62 \times 10^{-11} \text{ergcm}^{-2}\text{s}^{-1}$$

$$\log \frac{M_{BH}}{M_{\odot}} = 8.07 \pm 0.02 \quad F_{20-100\text{keV}} = 8.46 \times 10^{-11} \text{ergcm}^{-2}\text{s}^{-1}$$



Suzaku+Swift BAT best-fit model in the whole 0.6-150 keV band, and contour plot (Bianchi et al., 2010)

- **Suzaku + Swift BAT** (Bianchi et al., 2010; Mantovani et al., 2016): relativistic FeK α line + narrow component with no associated reflection component + Fe XXVI line emission;
- **ASCA and OSSE** (Grandi 1998): absorbed power law, $\Gamma=1.73$ & $E_c \sim 250$ keV + reflection component + cold iron line;
- **BeppoSAX** (Perola 2000): $\Gamma=1.84 \pm 0.05$ & $E_c = 169_{-78}^{+318}$ keV;
- **XMM-Newton** (Matt et al., 2006): lack of a soft excess + a large reflection component + narrow iron line + Fe XXVI line emission.

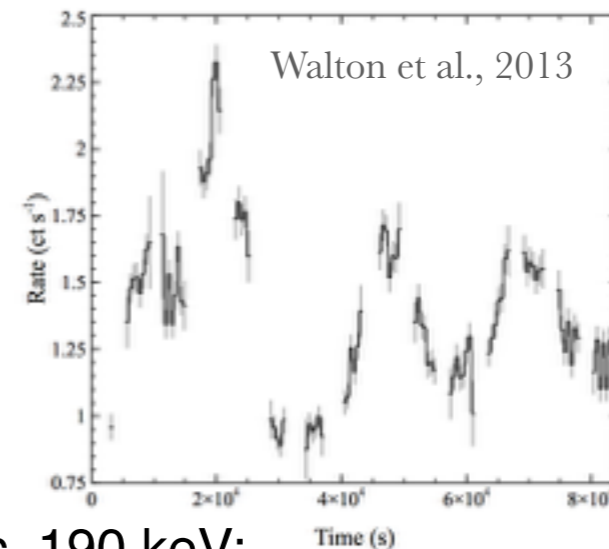


NGC 6814

$$z = 0.0052$$

$$F_{2-10\text{keV}} = 0.17 \times 10^{-11} \text{ergcm}^{-2}\text{s}^{-1}$$

$$\log \frac{M_{BH}}{M_{\odot}} = 6.99_{-0.25}^{+0.32} \quad F_{20-100\text{keV}} = 5.66 \times 10^{-11} \text{ergcm}^{-2}\text{s}^{-1}$$



0.5-10 keV XIS light curve for the Suzaku observation (Walton et al., 2013)

- **INTEGRAL** (Malizia et al., 2014): quite flat spectrum $\Gamma=1.68$ & $E_c \sim 190$ keV;
- **XMM-Newton** (Ricci et al., 2014): FeK α line with $EW \sim 84$ eV;
- **Suzaku** (Walton et al., 2013): no soft excess, fairly hard photon index $\Gamma=1.53$, variability.

NuSTAR Observation

MCG +8-11-11

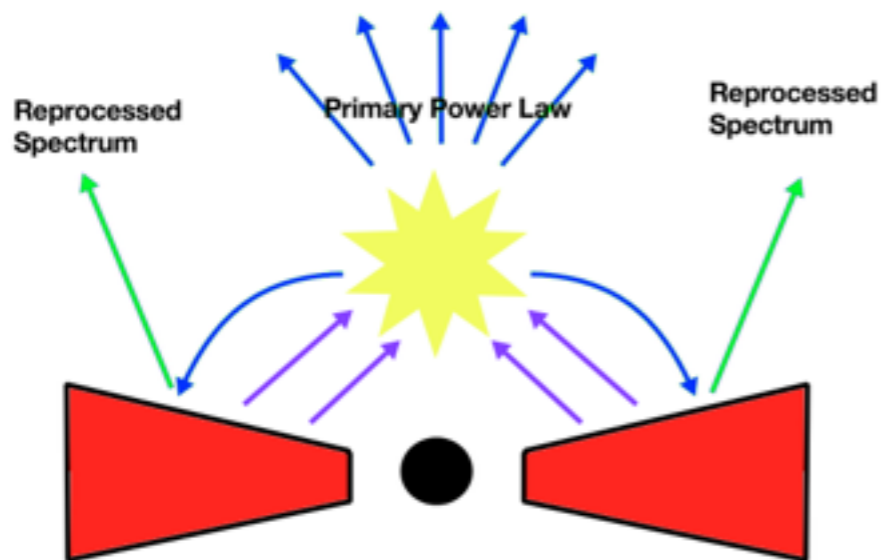
NGC 6814

100 ks observation in the *NuSTAR* AO2
(on 2016, August 19)

150 ks observation in the *NuSTAR* AO2
(on 2016, July, 04)

- Why? To investigate the Comptonization mechanisms acting in the innermost regions of AGN and which are believed to be responsible for the X-ray emission;
- *NuSTAR* (Nuclear Spectroscopic Telescopic Array) works in the band 3 - 79 keV;
- First focusing hard X-ray (10-79 keV) telescope in orbit;
- ~100 times more sensitive in the 10-79 keV band than any previous mission working in this band;

AGN in X-Rays

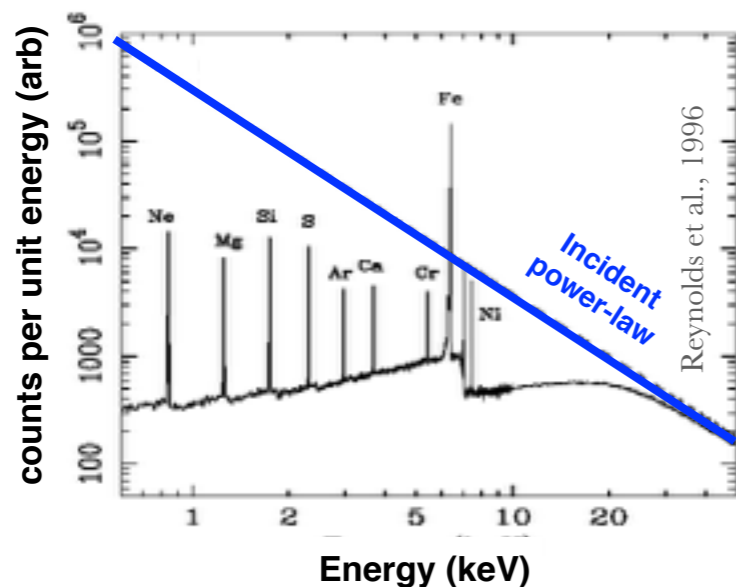
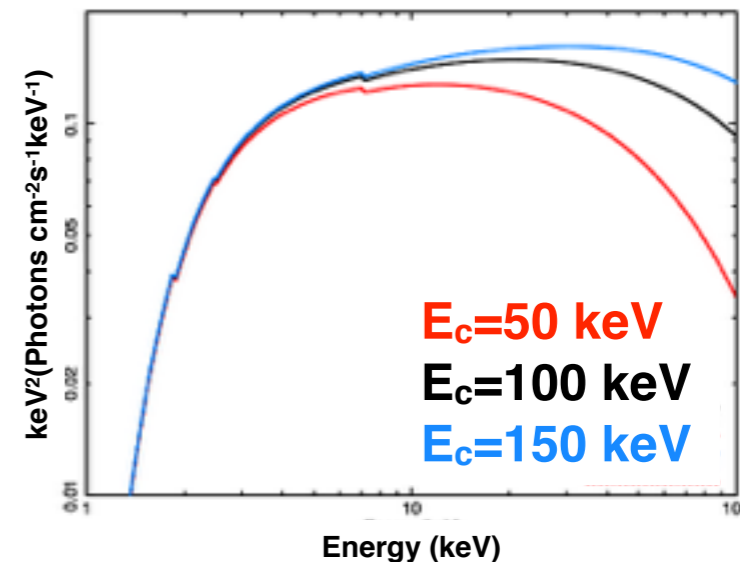


X-RAYS EMISSION:

In AGN the primary X-ray emission is due to Inverse Compton by electrons in a hot corona of the UV/soft X-ray disc photons.

PRIMARY POWER-LAW:

- Power-law with photon index and cutoff energy directly related to the temperature and to the optical depth of the coronal plasma.
- Most popular Comptonization models imply: $E_c = 2-3 \times kT_e$

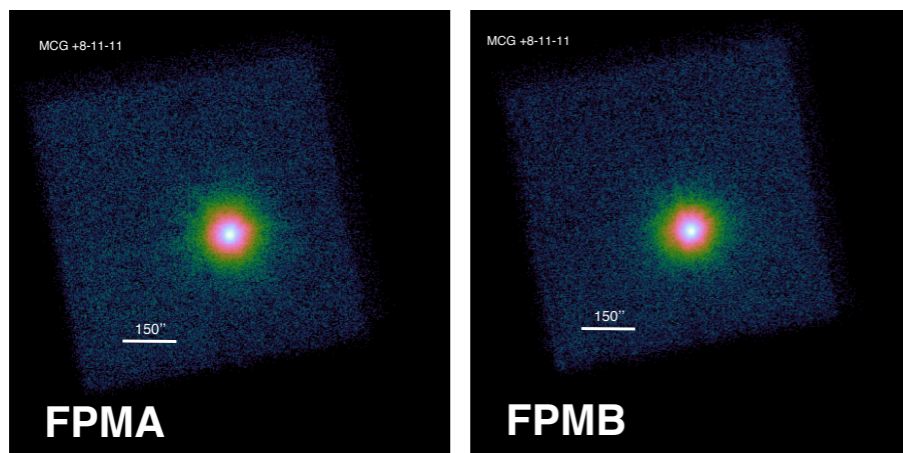


REPROCESSED EMISSION:

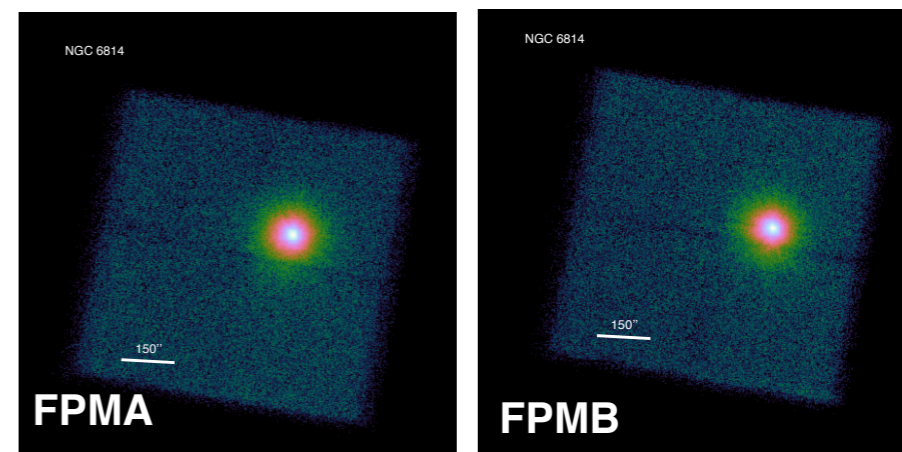
Typical X-ray features of the reflection by cold circumnuclear material include intense Fe K α line @ 6.4 keV and the associated Compton reflection continuum peaking @ $\sim 30 \text{ keV}$.

Analysis

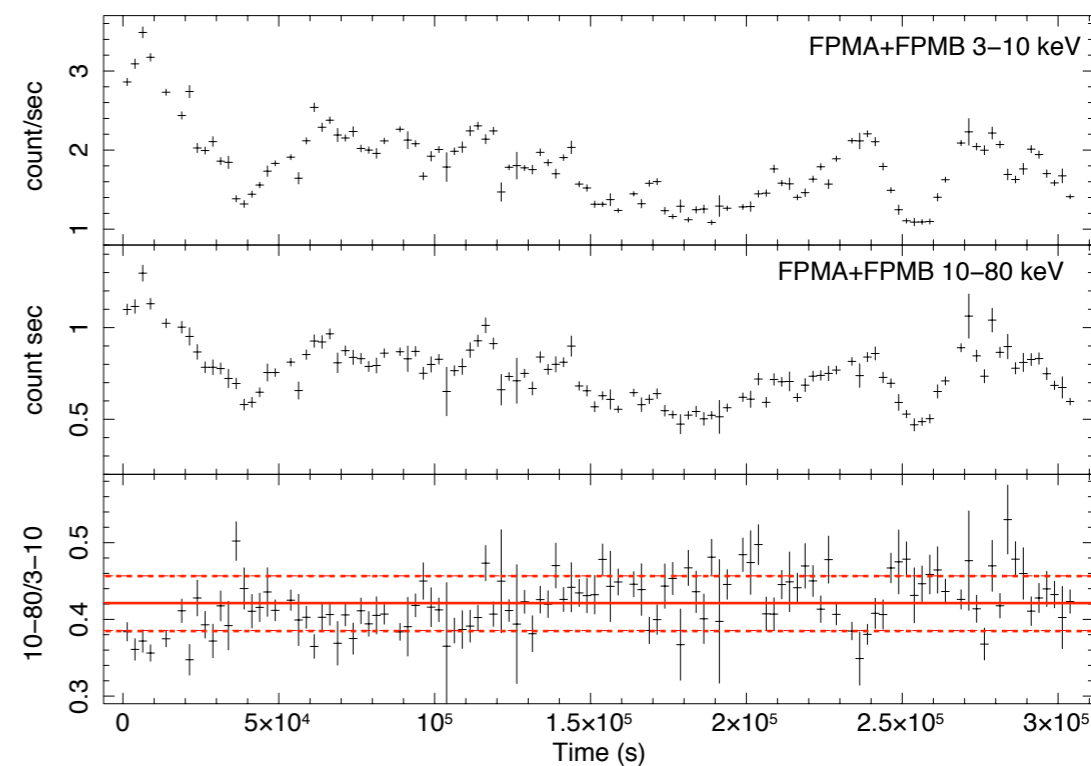
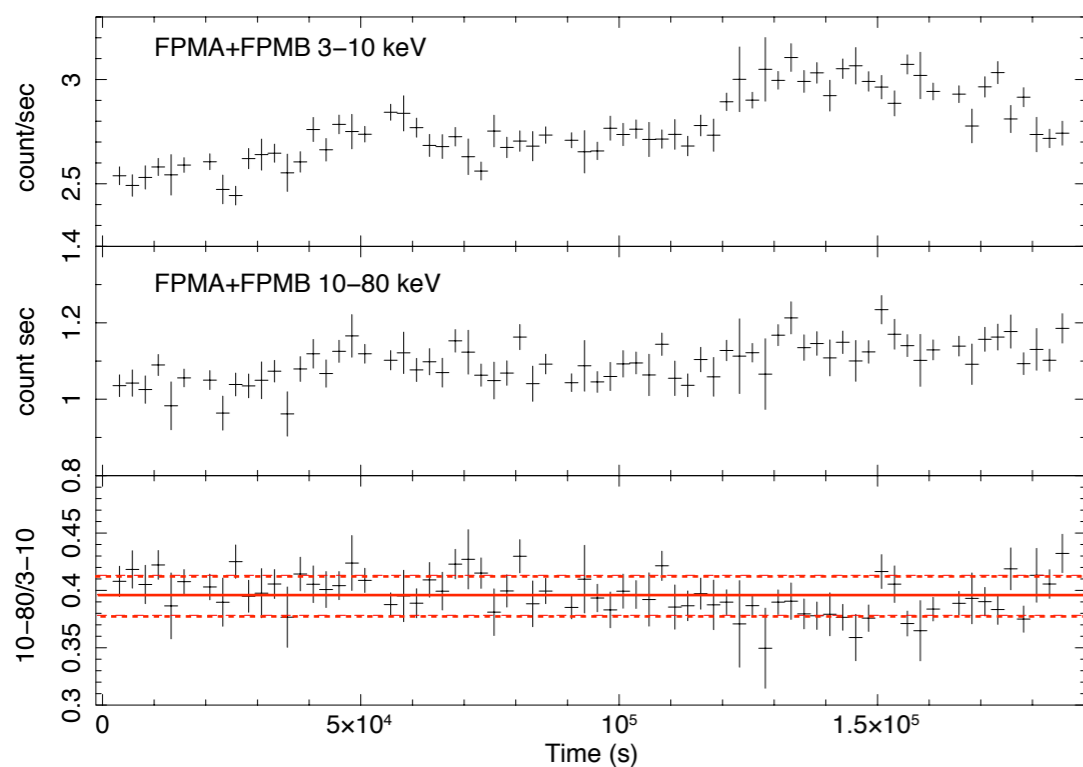
MCG +8-11-11



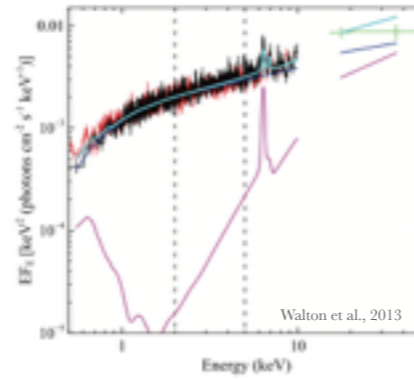
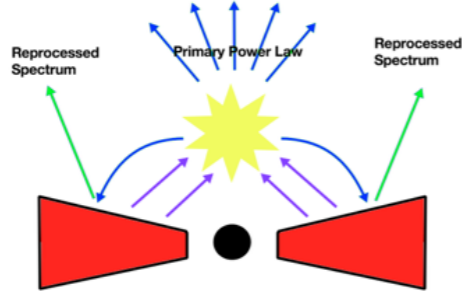
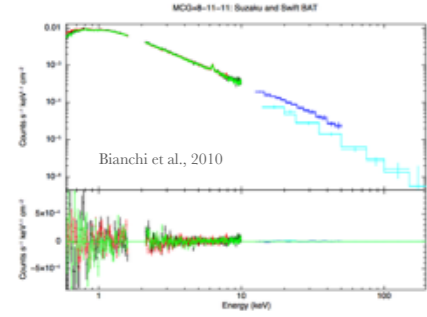
NGC 6814



Both sources show variability in their light curves but since no significant spectral variation is found in the ratio between the 10-80 and 3-10 keV count rates we used **time-averaged spectra** in our analysis.



Model



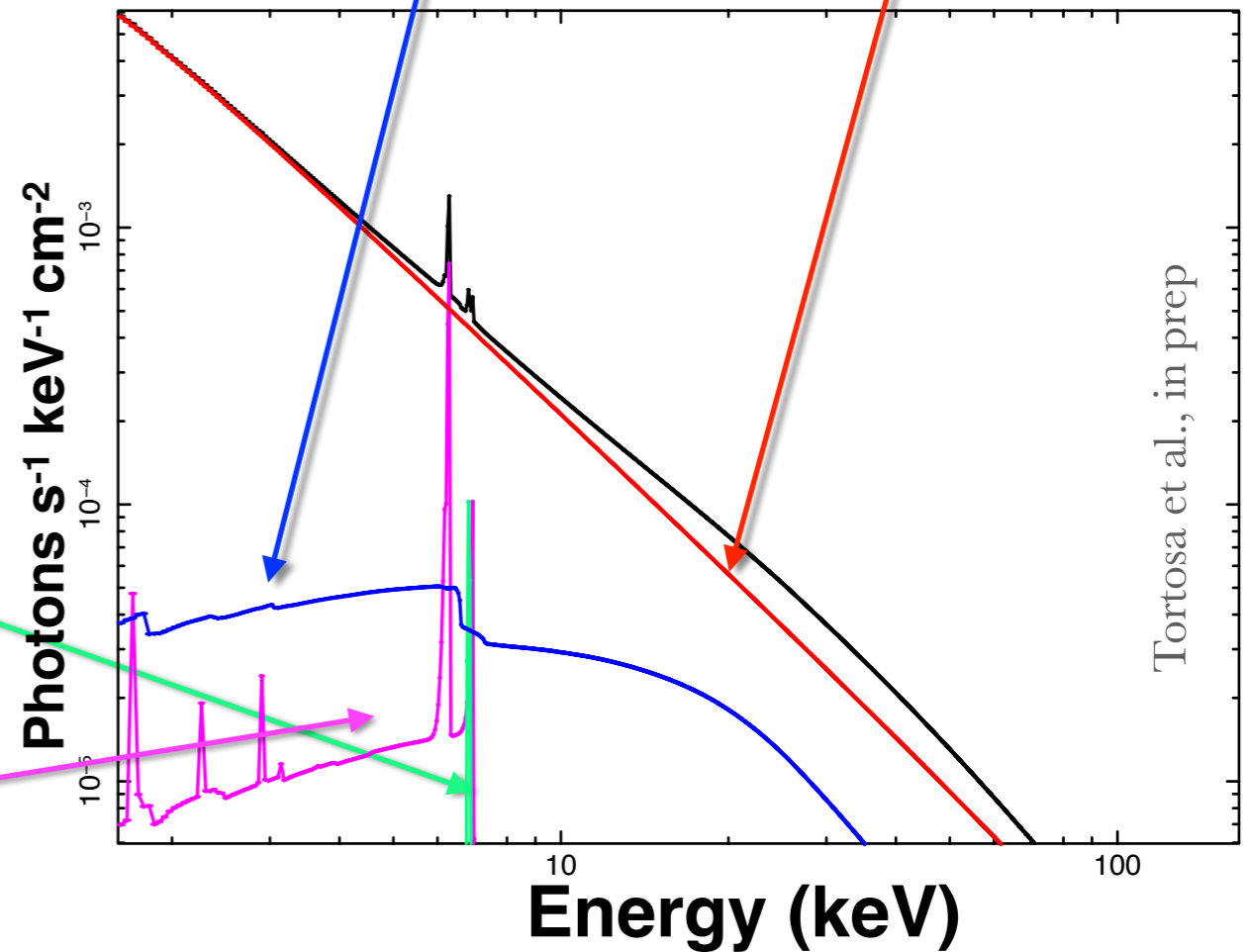
Relxill
(García et al. 2014)

Power law with exponential cutoff

- **Primary X-ray emission;**
- **Relativistic disk reflection;**
- **Cold, distant reflection;**
- **Narrow Fe XXVI line**
- **@ 6.966 keV (MCG +8-11-11)**

Fe XXVI - ZGAUSS

Xillver
(García & Kallman 2010;
García et al. 2013)



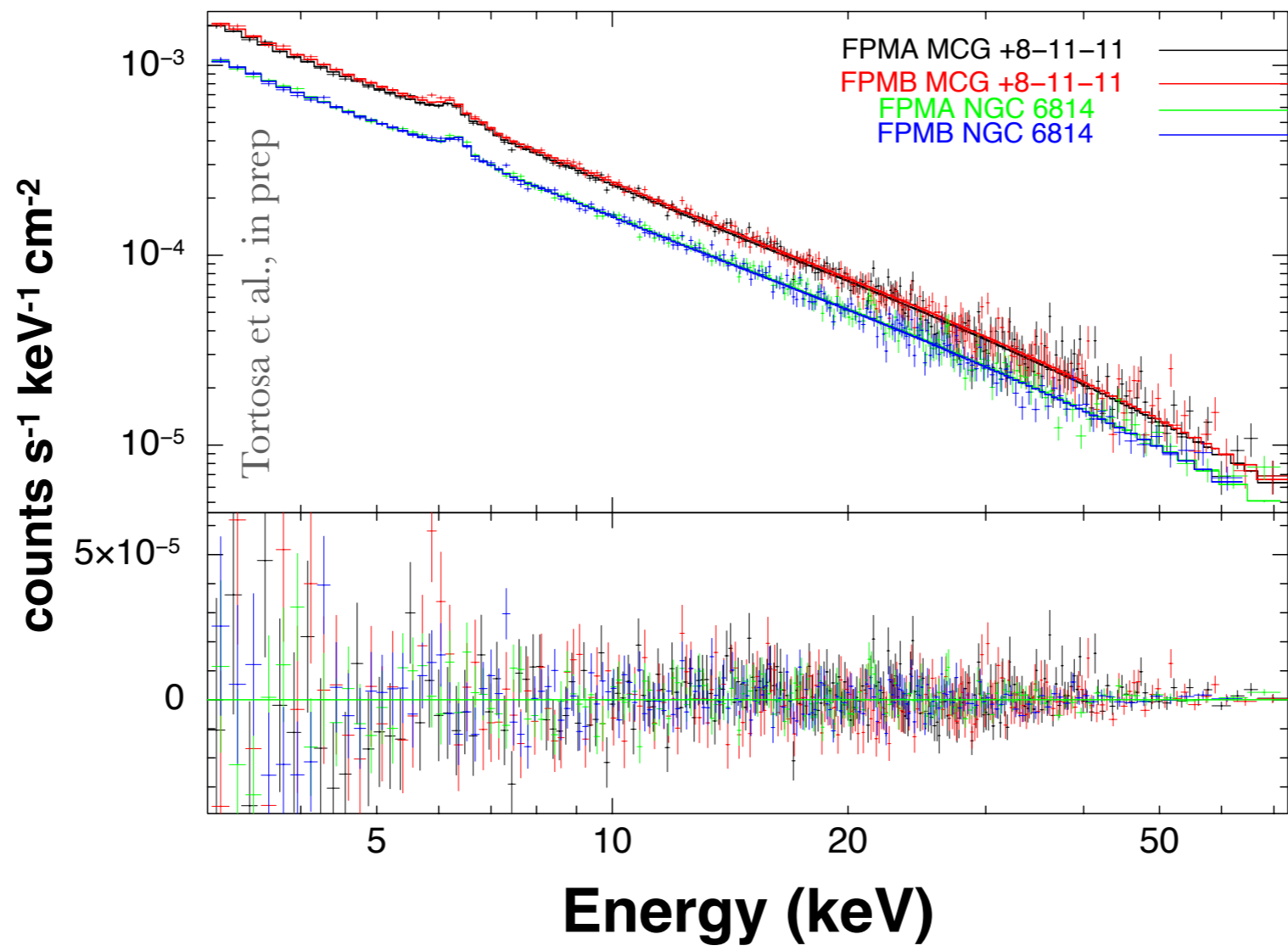
Spectral Parameters

MCG +8-11-11

$$\Gamma = 1.77 \pm 0.04$$
$$E_c = 175^{+110}_{-50} \text{ keV}$$
$$R^{\text{refl}} = 0.25 \pm 0.12$$

NGC 6814

$$\Gamma = 1.71^{+0.04}_{-0.03}$$
$$E_c = 155^{+70}_{-35} \text{ keV}$$
$$R^{\text{refl}} = 0.27^{+0.10}_{-0.12}$$



Spectral Parameters

MCG +8-11-11

$$\Gamma = 1.77 \pm 0.04$$

$$E_c = 175_{-50}^{+110} \text{ keV}$$

$$R^{\text{refl}} = 0.25 \pm 0.12$$

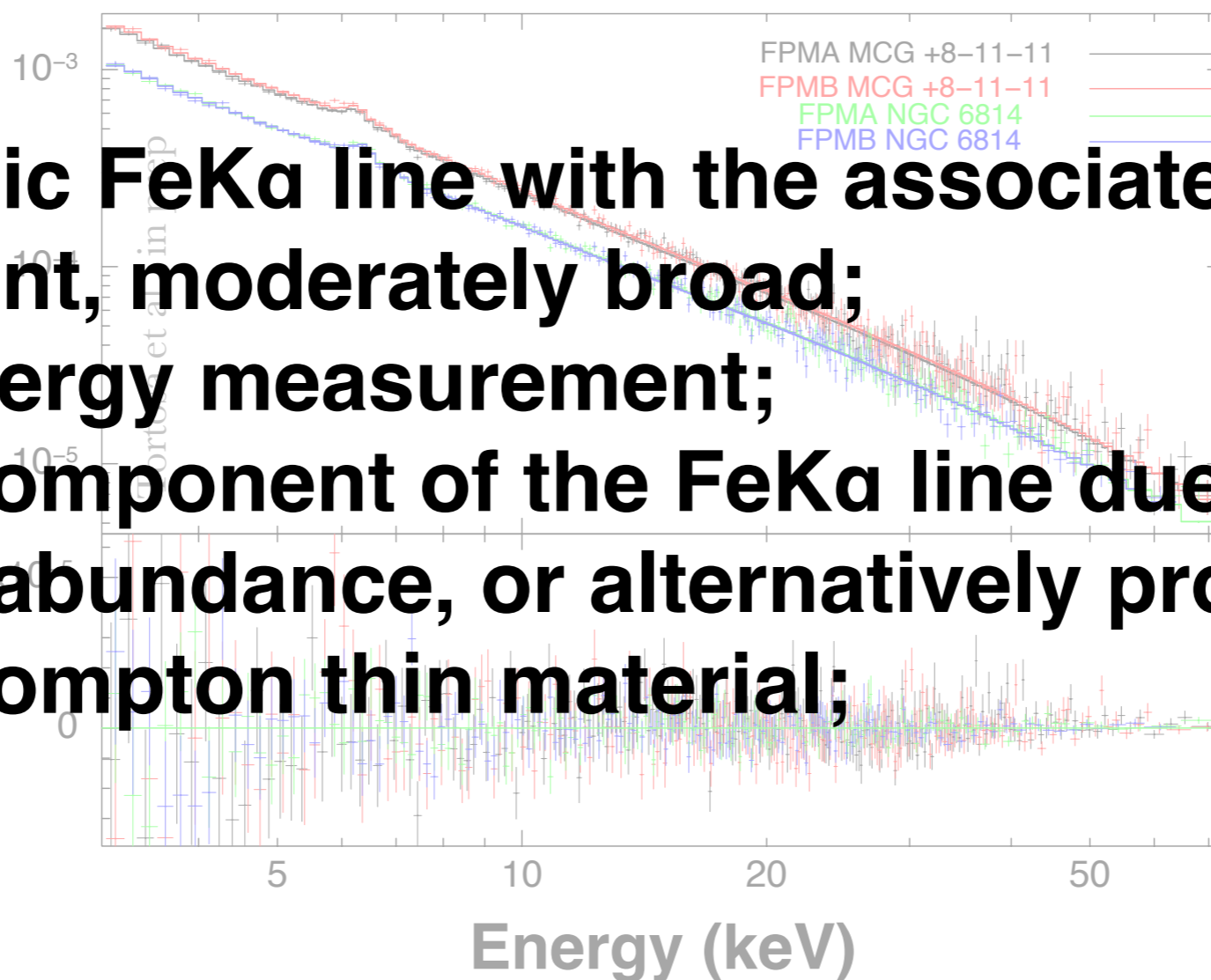
NGC 6814

$$\Gamma = 1.71_{-0.03}^{+0.04}$$

$$E_c = 155_{-35}^{+70} \text{ keV}$$

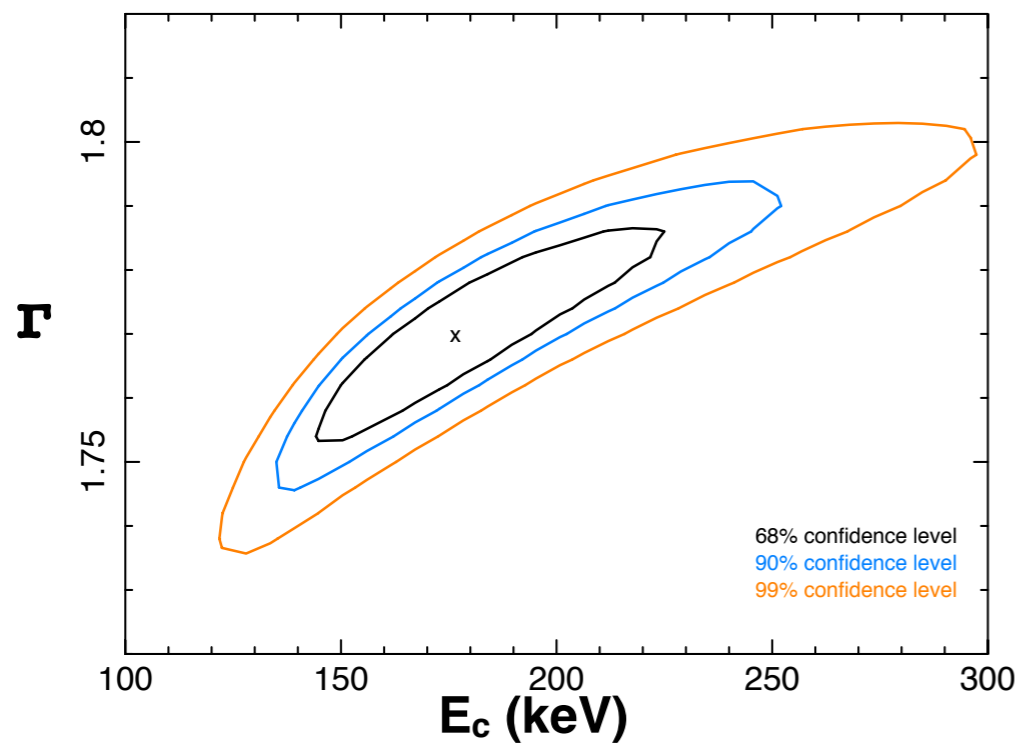
$$R^{\text{refl}} = 0.27_{-0.12}^{+0.10}$$

- * **Relativistic FeK α line with the associated reflection component, moderately broad;**
- * **Cutoff energy measurement;**
- * **Narrow component of the FeK α line due to a large iron overabundance, or alternatively produced in distant Compton thin material;**

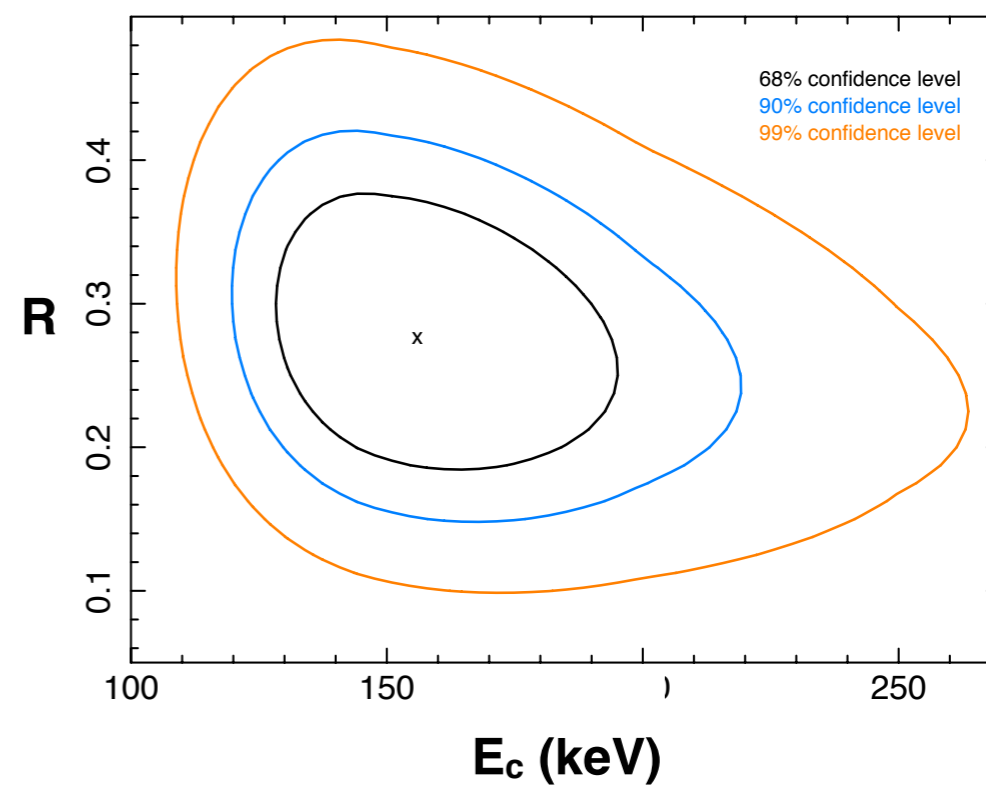
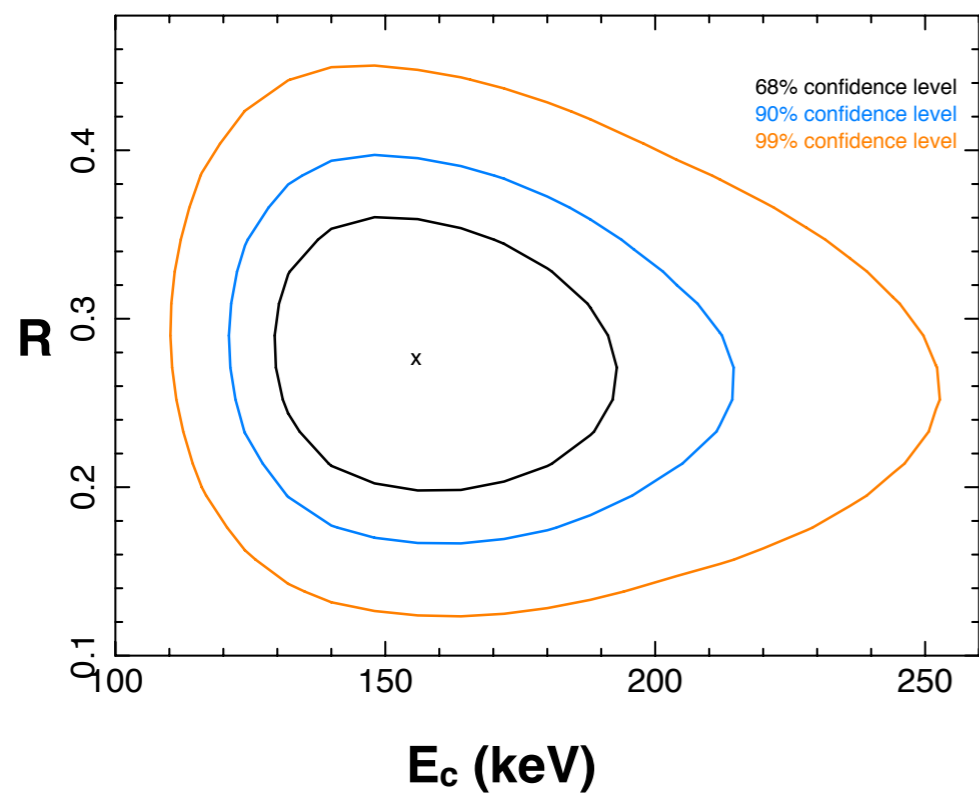
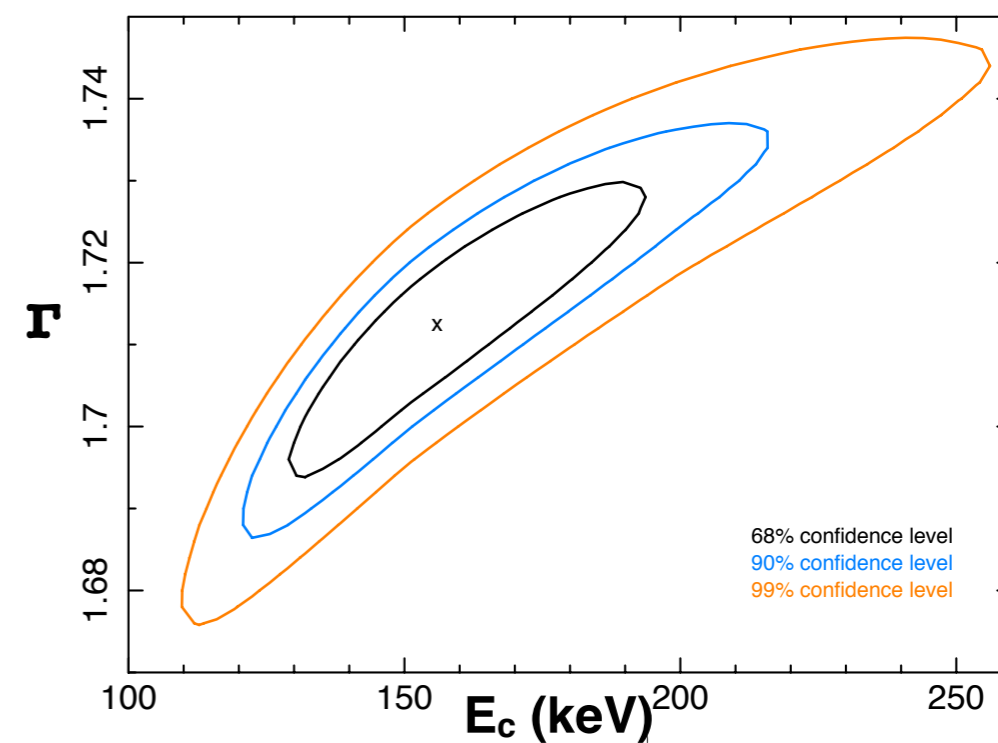


Spectral Parameters

MCG +8-11-11



NGC 6814



Coronal Parameters

The coronal temperature is expected to be related to the cutoff energy by $E_c = 2-3 \times kT_e$ (Petrucci 2000, 2001)

CompTT (Titarchuk et al., 1994) convolved with the **REFLECT** model in XSPEC (reflection from neutral material according to the method of Magdziarz & Zdziarski, 1995)

MCG +8-11-11

NGC 6814



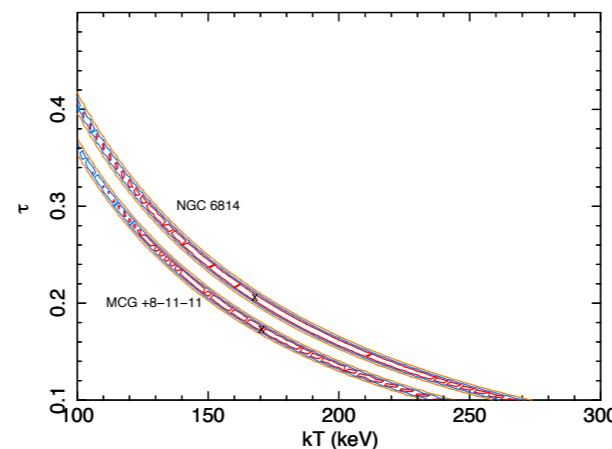
SLAB

$$kT = 170^{+150}_{-70} \text{ keV}$$

$$\tau = 0.17 \pm 0.1$$

$$kT = 165^{+100}_{-50} \text{ keV}$$

$$\tau = 0.2^{+0.30}_{-0.15}$$



SPHERE

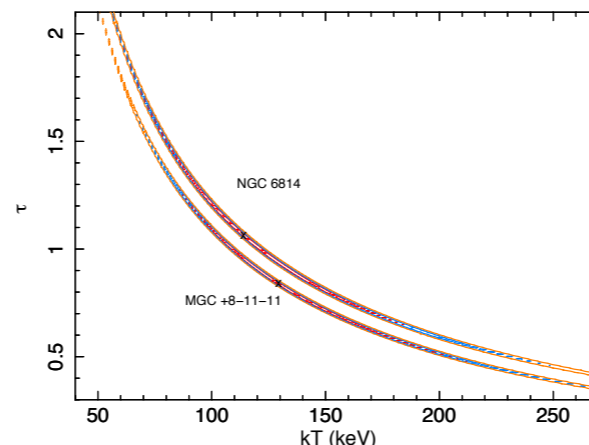
$$kT = 150^{+80}_{-70} \text{ keV}$$

$$\tau = 0.7^{+0.7}_{-0.3}$$



$$kT = 110^{+100}_{-70} \text{ keV}$$

$$\tau = 1.1^{+0.3}_{-0.8}$$



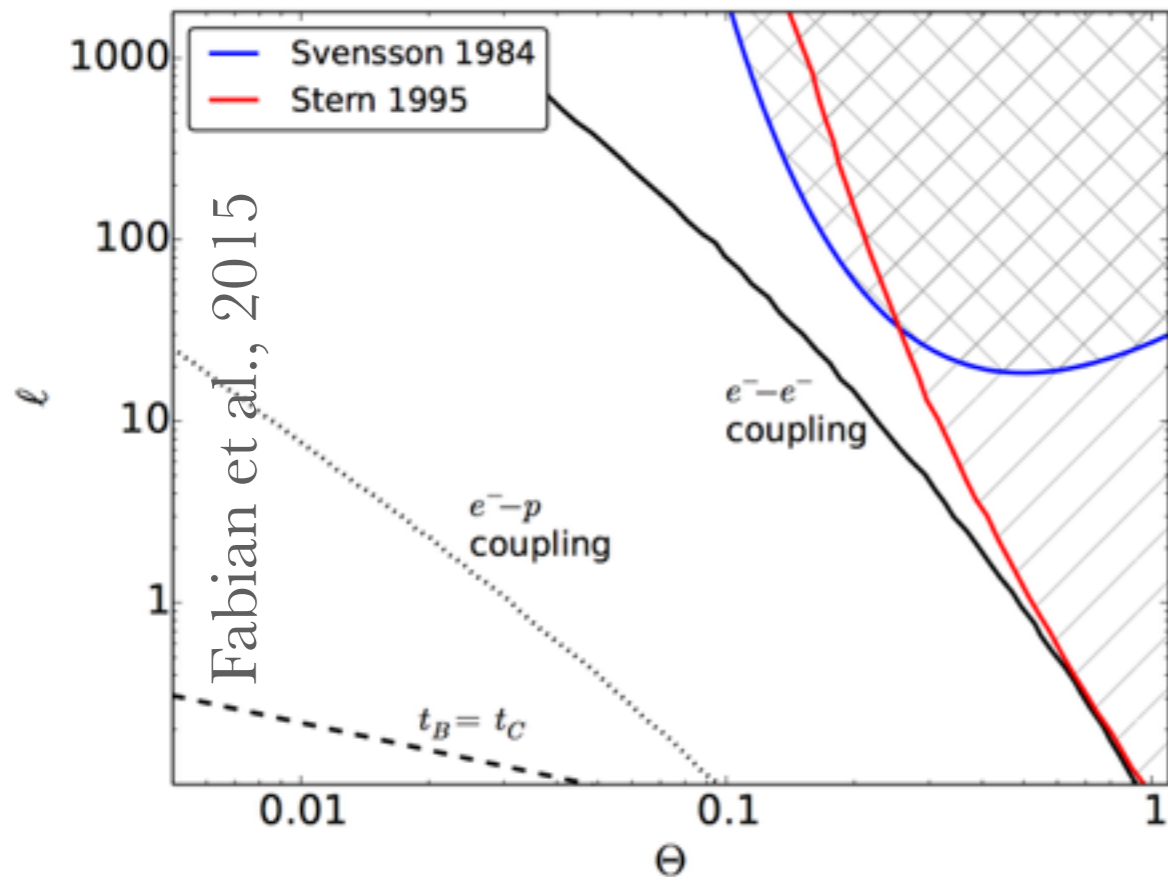
Θ - ℓ plane

Θ electron temperature normalized to the electron rest energy

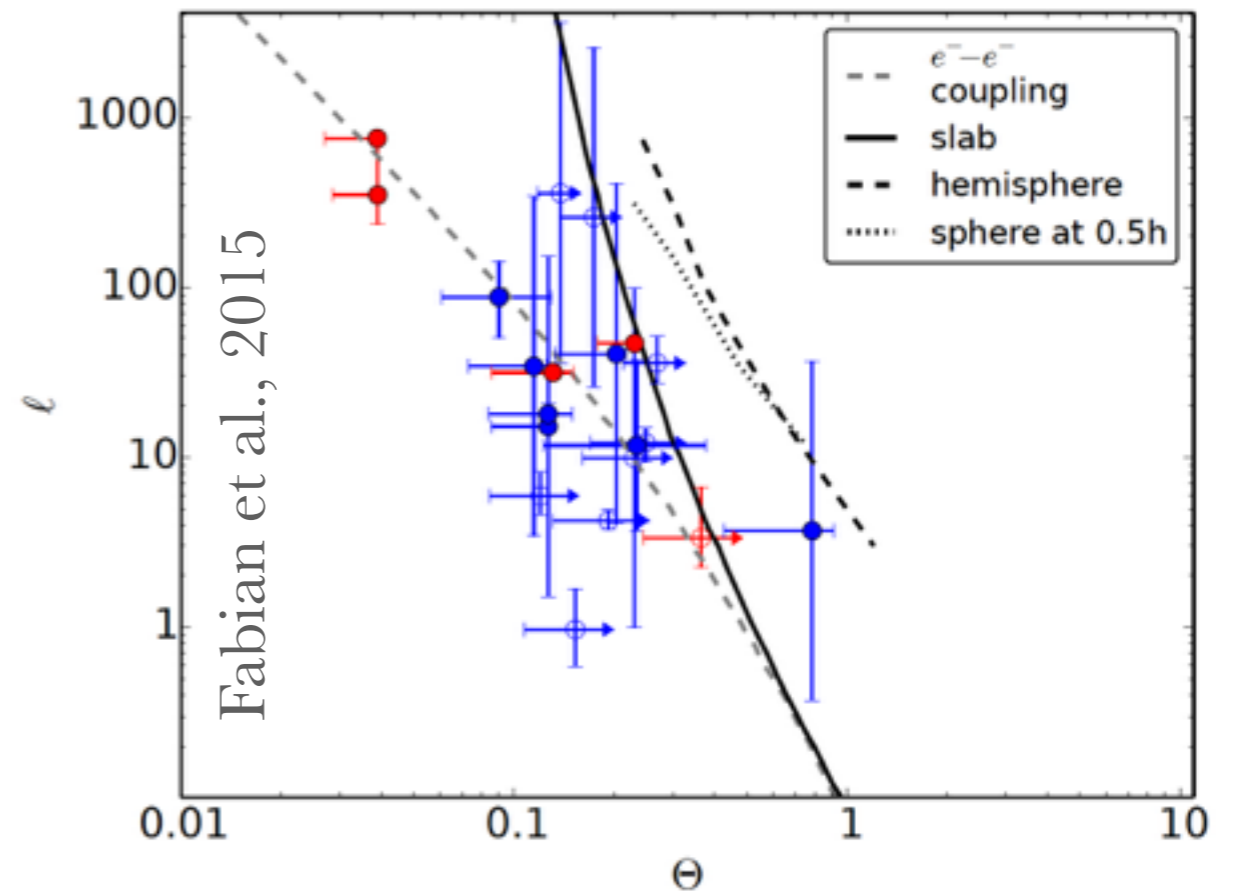
$$\Theta_e = \frac{kT_e}{m_e c^2}$$

ℓ the dimensionless compactness parameter

$$\ell = \frac{L}{R} \frac{\sigma_T}{m_e c^3}$$



Summary of the theoretical understanding of the Θ - ℓ plane.



Θ - ℓ distribution for *NuSTAR* observed AGN (blue points) and BHB (red points)

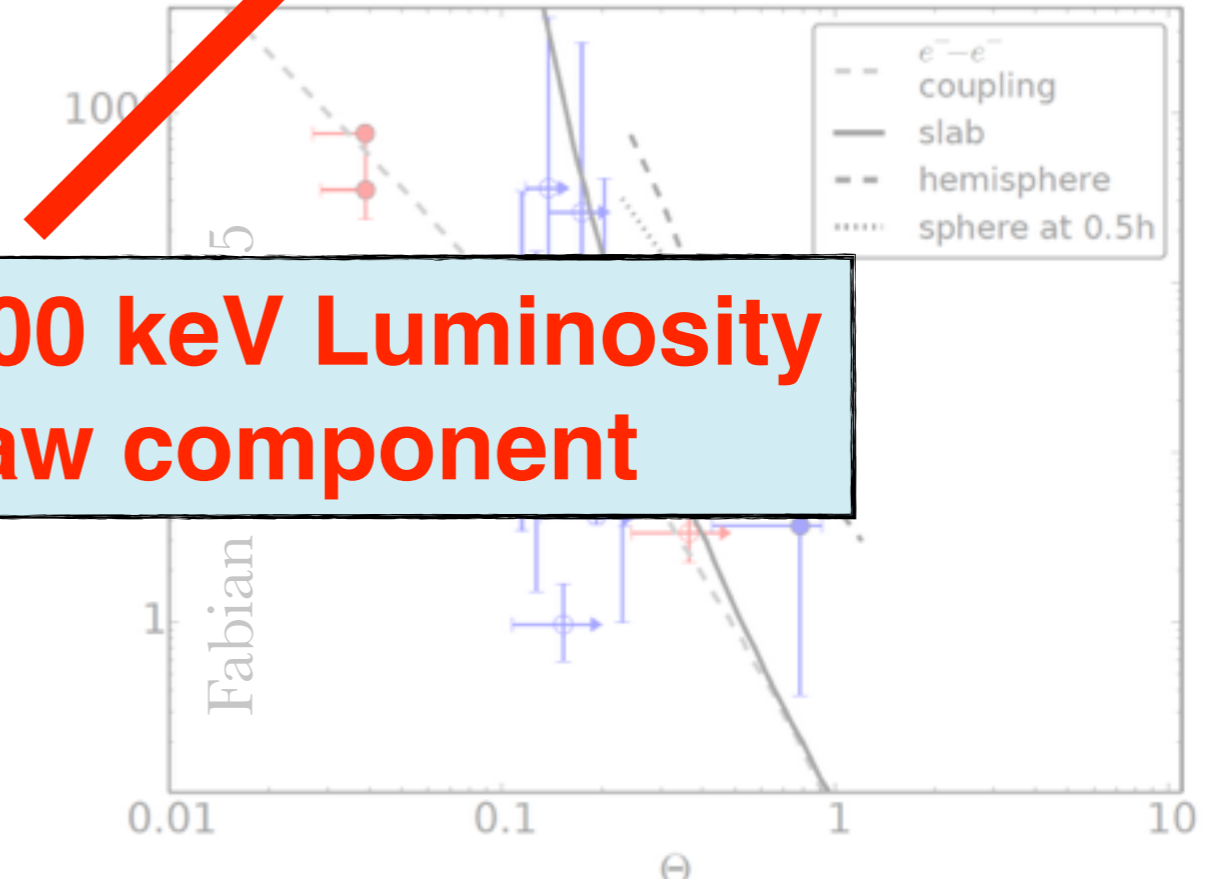
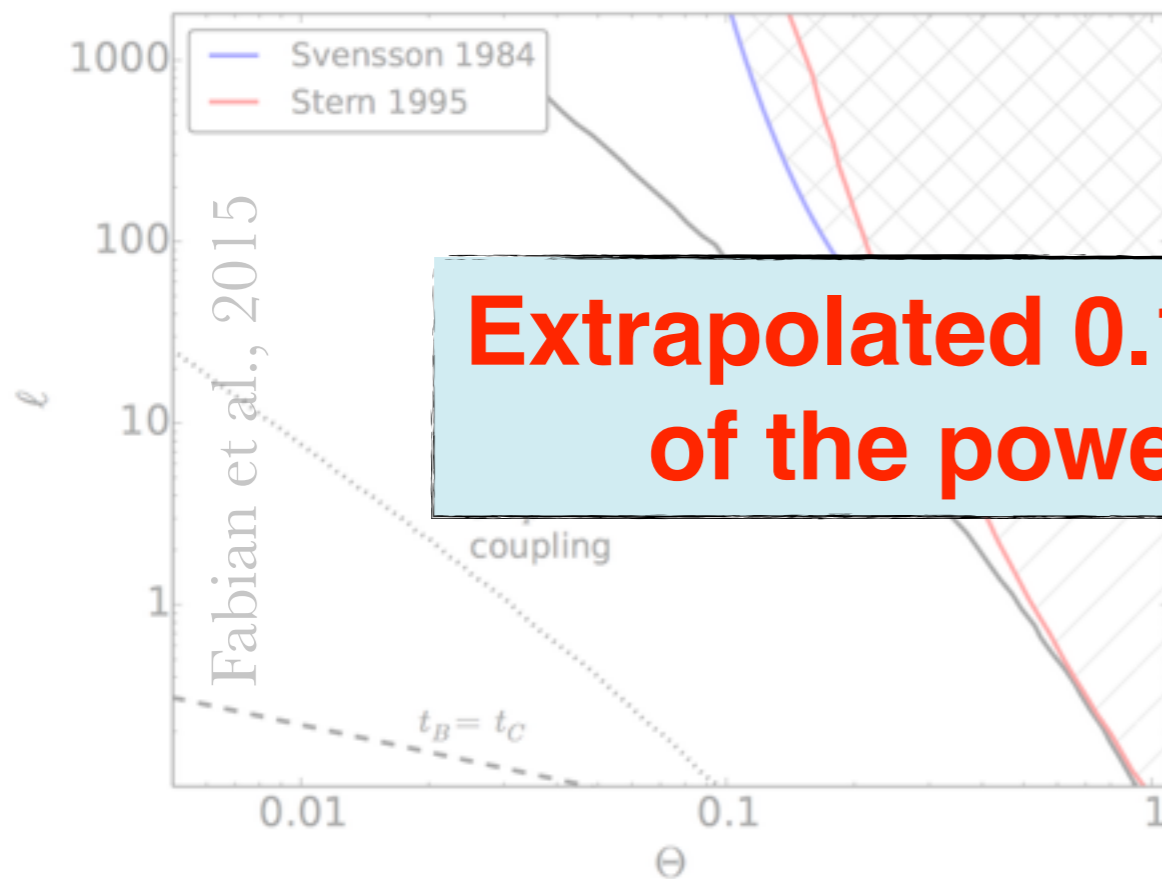
Θ - ℓ plane

Θ electron temperature normalized to the electron rest energy

$$\Theta_e = \frac{kT_e}{m_e c^2}$$

ℓ the dimensionless compactness parameter

$$\ell = \frac{L}{R} \frac{\sigma_T}{m_e c^3}$$



Extrapolated 0.1-200 keV Luminosity of the power-law component

Summary of the theoretical understanding of the plane.

Θ - ℓ points) and BHB (red points)

Θ - ℓ plane

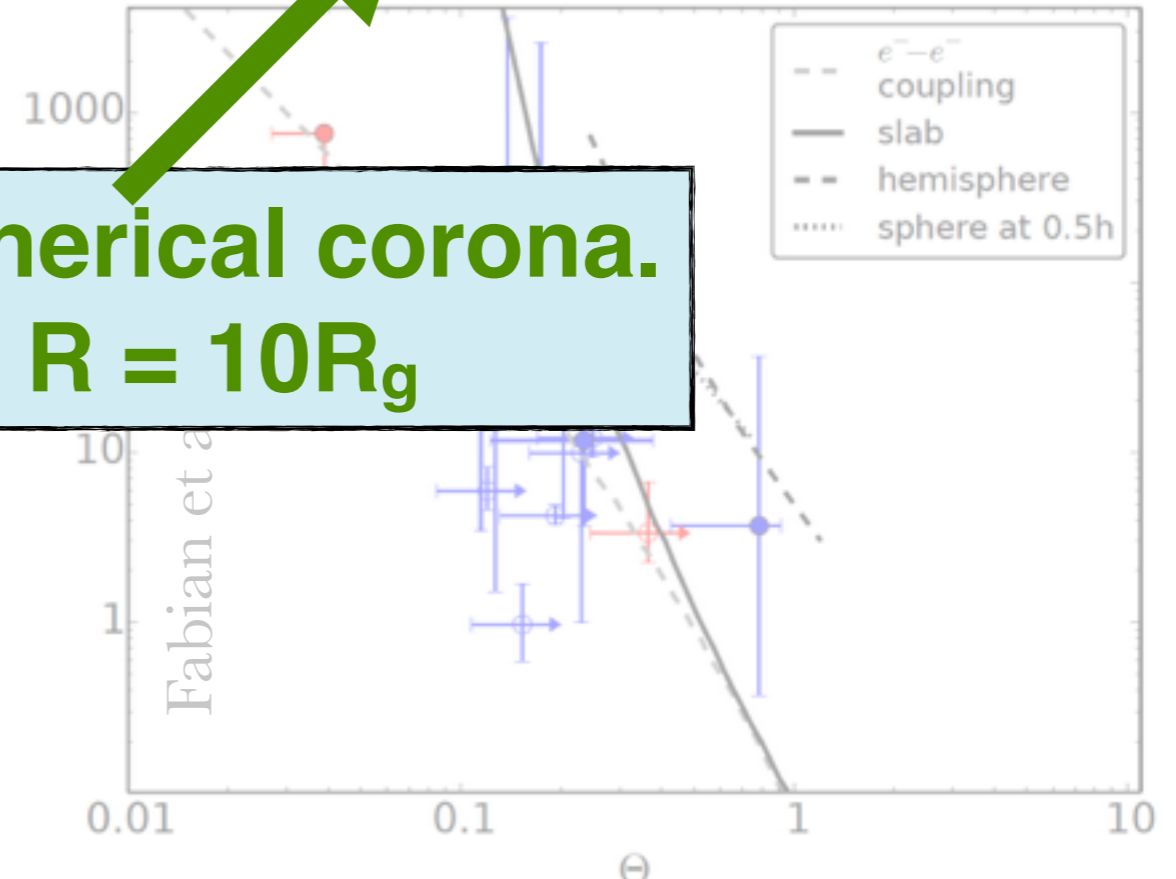
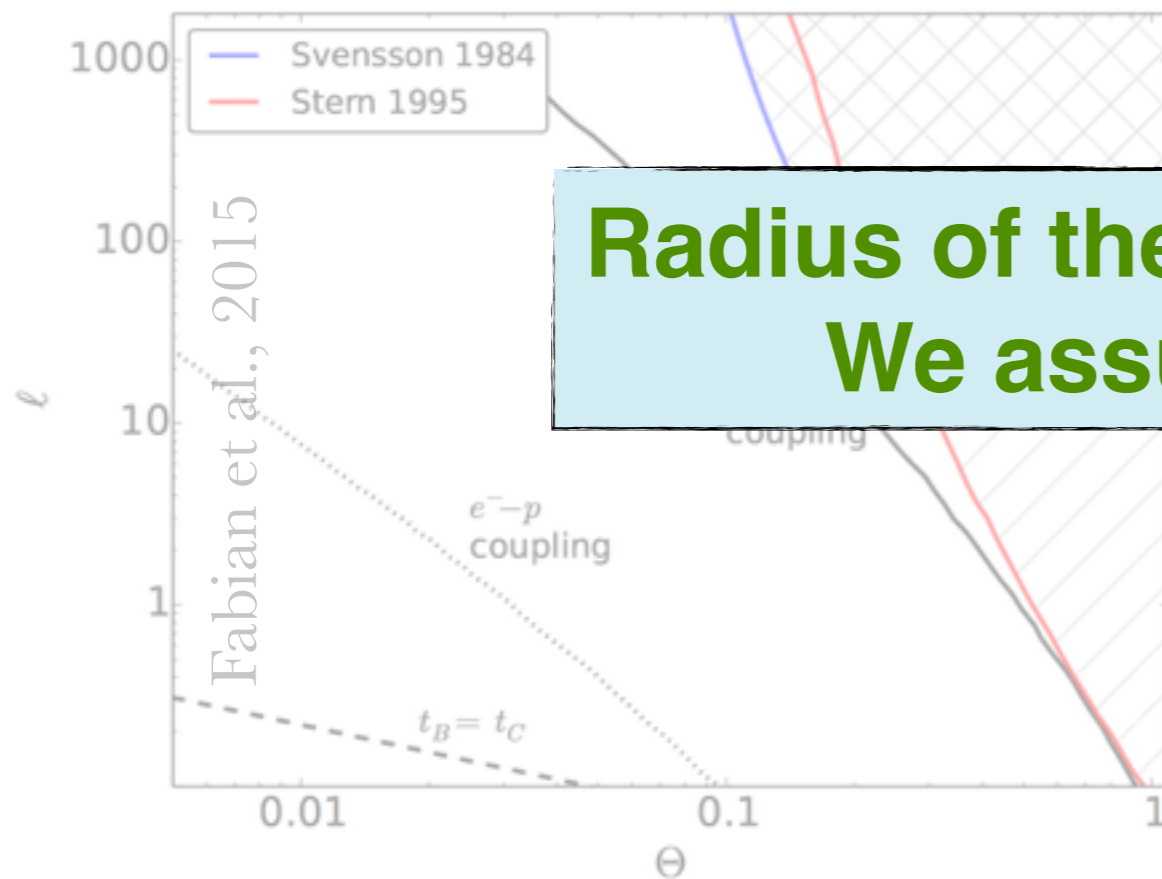
Θ electron temperature normalized to the electron rest energy

$$\Theta_e = \frac{kT_e}{m_e c^2}$$

ℓ the dimensionless compactness parameter

$$\ell = \frac{L \sigma_T}{\mathbf{R} m_e c^3}$$

**Radius of the spherical corona.
We assume $R = 10R_g$**



Summary of the theoretical understanding of the Θ - ℓ plane.

Θ - ℓ plane (blue points) and BHB (red points)

Θ - ℓ plane

MCG +8-11-11

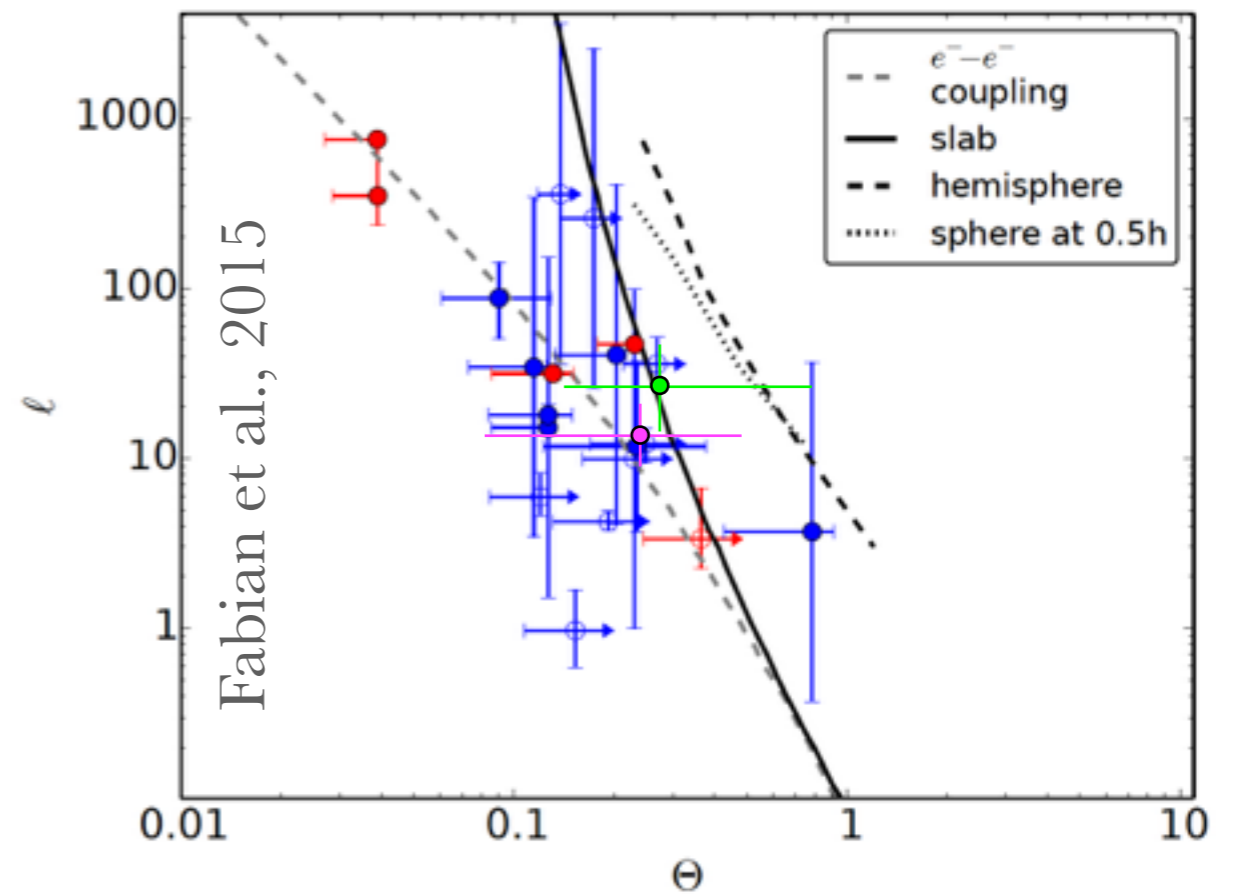
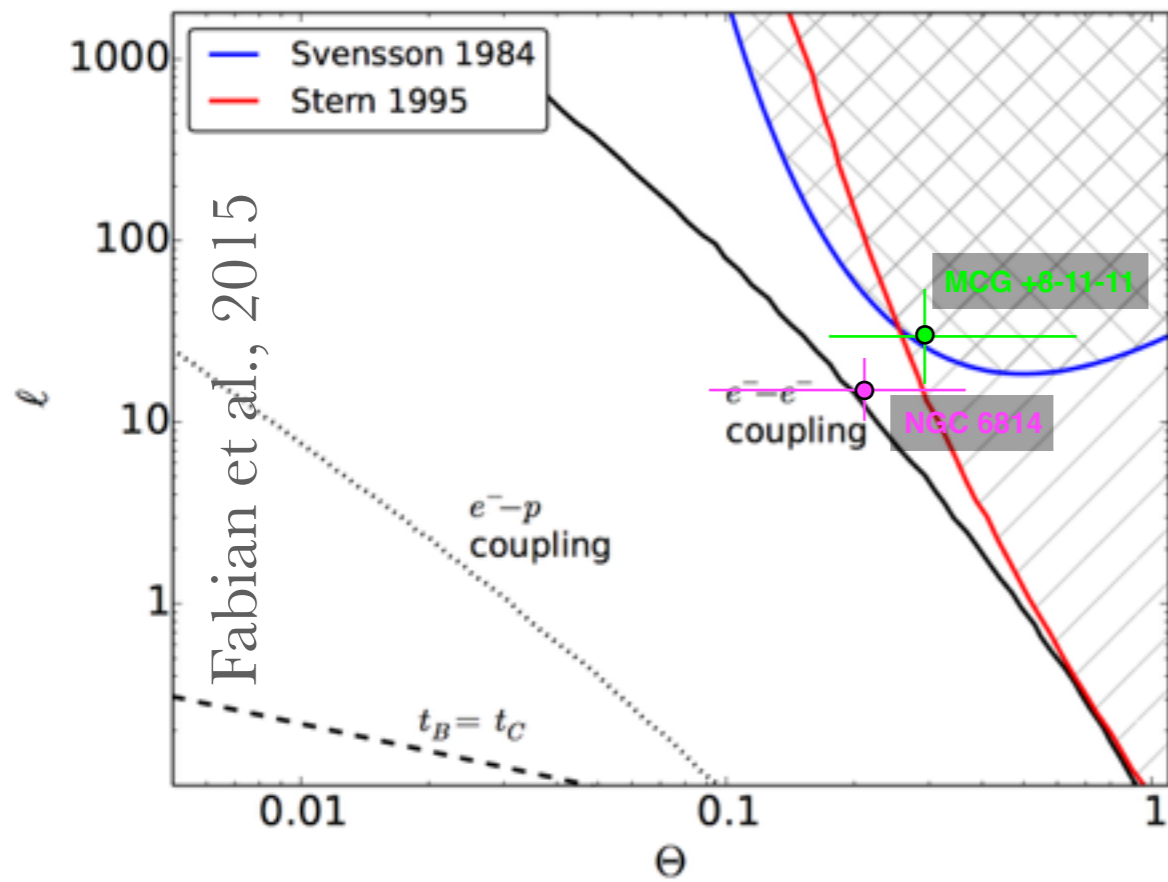
$$\Theta_e = 0.28^{+0.28}_{-0.11}$$

$$\ell = 27 \pm 12 (R_{10})^{-1}$$

NGC 6814

$$\Theta_e = 0.22^{+0.15}_{-0.12}$$

$$\ell = 14.5 \pm 4.5 (R_{10})^{-1}$$



Summary of the theoretical understanding of the Θ - ℓ plane.

Θ - ℓ distribution for *NuSTAR* observed AGN (blue points) and BHB (red points)

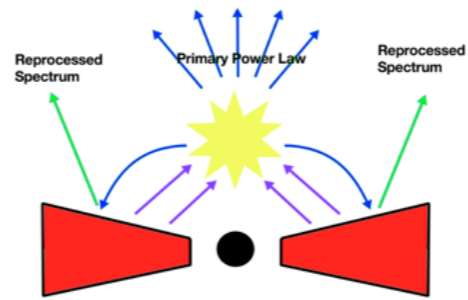
Looking for correlations

Unobscured nearby Seyfert Galaxies observed by *NuSTAR*

Source	Γ	E_c [keV]	$\log(M_{\text{bh}}/M_{\odot})$	$L_{\text{bol}}/L_{\text{Edd}}$	$L_{2-10\text{keV}} \times 10^{44} \text{ ergs s}^{-1}$	Ref.
NGC 5506	1.91 ± 0.03	720^{+130}_{-190}	8.0 ± 0.2	6.21×10^{-3}	0.0526	1 - 2
MCG 5-23-16	1.85 ± 0.01	166^{+6}_{-5}	7.2 ± 0.2	3.73×10^{-2}	0.166	3 - 4
SWIFT J2127.4+5654	2.08 ± 0.01	108^{+11}_{-10}	7.2 ± 0.2	1.02×10^{-1}	0.133	5 - 6
IC4392A	1.73 ± 0.01	184 ± 14	8.2 ± 0.1	9.8×10^{-2}	0.626	7 - 8
3C390.3	1.70 ± 0.01	116^{+24}_{-8}	9.04 ± 0.4	5.17×10^{-2}	1.8	9 - 10
3C 382	$1.68^{+0.03}_{-0.02}$	214^{+147}_{-63}	7.7 ± 0.5	5.06×10^{-2}	2.3	11 - 12
GRS 1734-292	1.65 ± 0.05	53^{+11}_{-8}	8.5 ± 0.1	3.3×10^{-2}	0.056	13
NGC 6814	$1.71^{+0.04}_{-0.03}$	135^{+70}_{-35}	7.2 ± 0.05	1.22×10^{-2}	0.0204	9-14
MCG +8-11-11	1.77 ± 0.04	175^{+110}_{-50}	8.07 ± 0.02	9.59×10^{-2}	0.513	14 - 15
Ark 564	2.27 ± 0.08	42 ± 3	6.4 ± 0.5	1.1	0.39	16 - 17
PG 1247+267	$2.35^{+0.09}_{-0.08}$	89^{+134}_{-34}	$8.3^{+0.17}_{-0.15}$	1.16×10^{-2}	0.15	18 - 19
NGC 7213	1.84 ± 0.03	> 140	8.0 ± 0.2	1.03×10^{-3}	0.012	20 - 21
MCG 6-30-15	2.06 ± 0.01	> 110	6.2 ± 0.1	1.20×10^{-1}	0.02	22 -23
NGC 2110	1.65 ± 0.03	> 210	8.3 ± 0.2	9.78×10^{-5}	0.004	24 - 25
Mrk 335	$2.14^{+0.02}_{-0.04}$	> 174	7.1 ± 0.01	2.32×10^{-1}	0.18	26 - 27
Ark 120	1.73 ± 0.02	> 190	8.2 ± 0.1	1.25×10^{-1}	0.56	26 - 28
Fairall 9	$1.96^{+0.01}_{-0.02}$	> 242	6.8 ± 0.02	7.57×10^{-2}	0.77	26 - 29
Mrk766	$2.22^{+0.02}_{-0.03}$	> 441	$6.8^{+0.05}_{-0.06}$	8.34×10^{-2}	0.046	30 -31
PG1211+143	2.51 ± 0.2	> 124	$8.16^{+0.11}_{-0.16}$	4.76×10^{-2}	0.35	26 -32

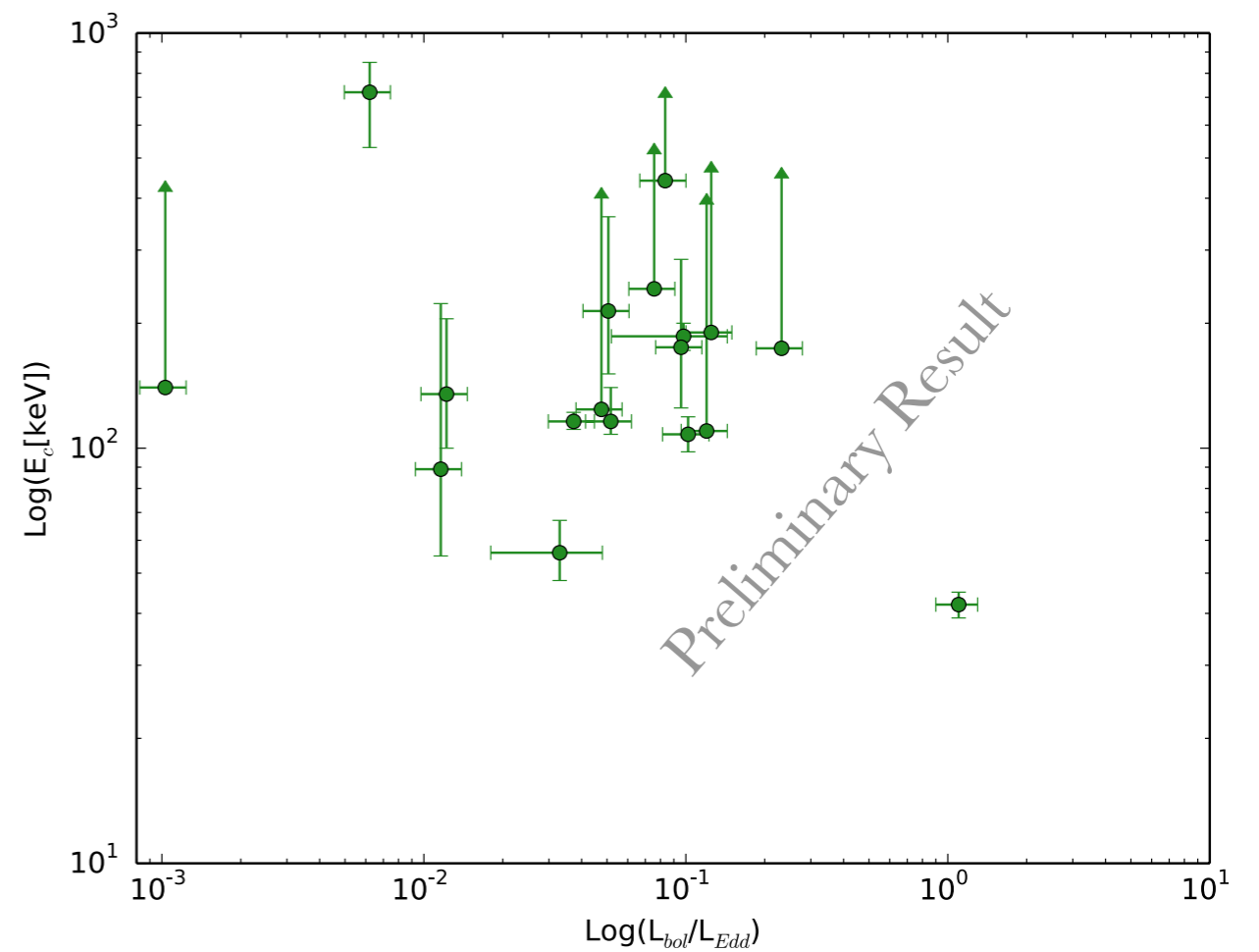
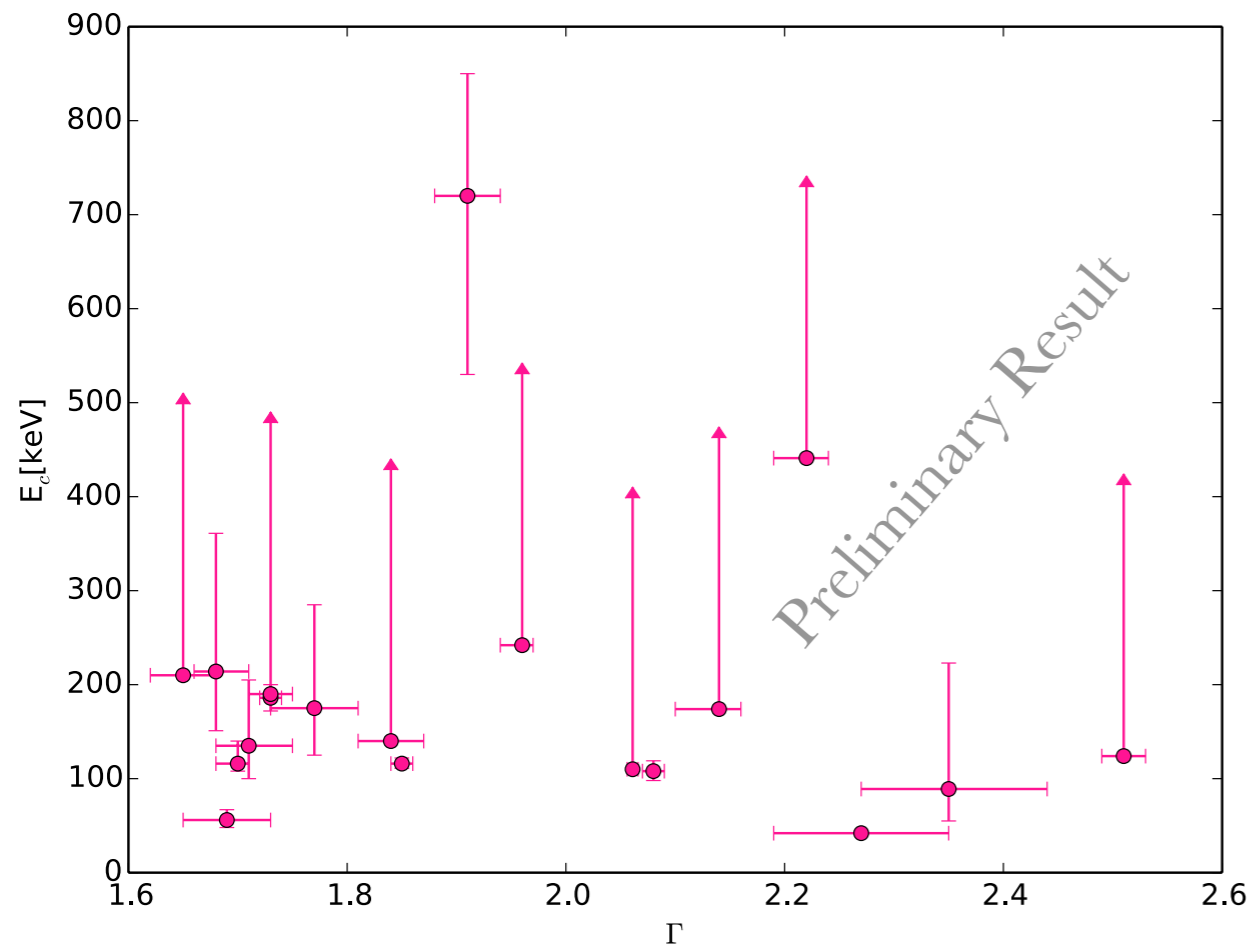
References: 1. Matt et al. (2015), 2. Guainazzi et al. (2010), 3. Ponti et al. (2012), Baloković et al. (2015), 5. Marinucci et al. (2014a), 6. Malizia et al. (2008), 7. Bianchi et al. (2009), 8. Brenneman et al. (2014), 9. Grier et al. (2013), 10. Lohfink et al. (2015), 11. Winter et al. (2009) 12. Ballantyne et al. (2014), 13. Tortosa et al. (2017), 14. Tortosa et al., in prep., 15. Winter et al. (2010), 16. Kara et al. (2017), 17. Zhang & Wang (2006), 18. Lanzuisi et al. (2016), 19. Trevese et al. (2014), 20. Ursini et al. (2015), 21. Blank et al. (2005), 22. Marinucci et al. (2014b), 23. Emmanoulopoulos et al. (2014), 24. Marinucci et al. (2015), 25. Moran et al. (2007), 26. Peterson et al. (2004), 27. Grier et al. (2012), 28. Matt et al. (2014), 29. Lohfink et al. (2016), 30. Buisson et al. (2017), 31. Bentz et al. (2010), 32. Zoghbi et al. (2015).

Looking for correlations



Photon Index

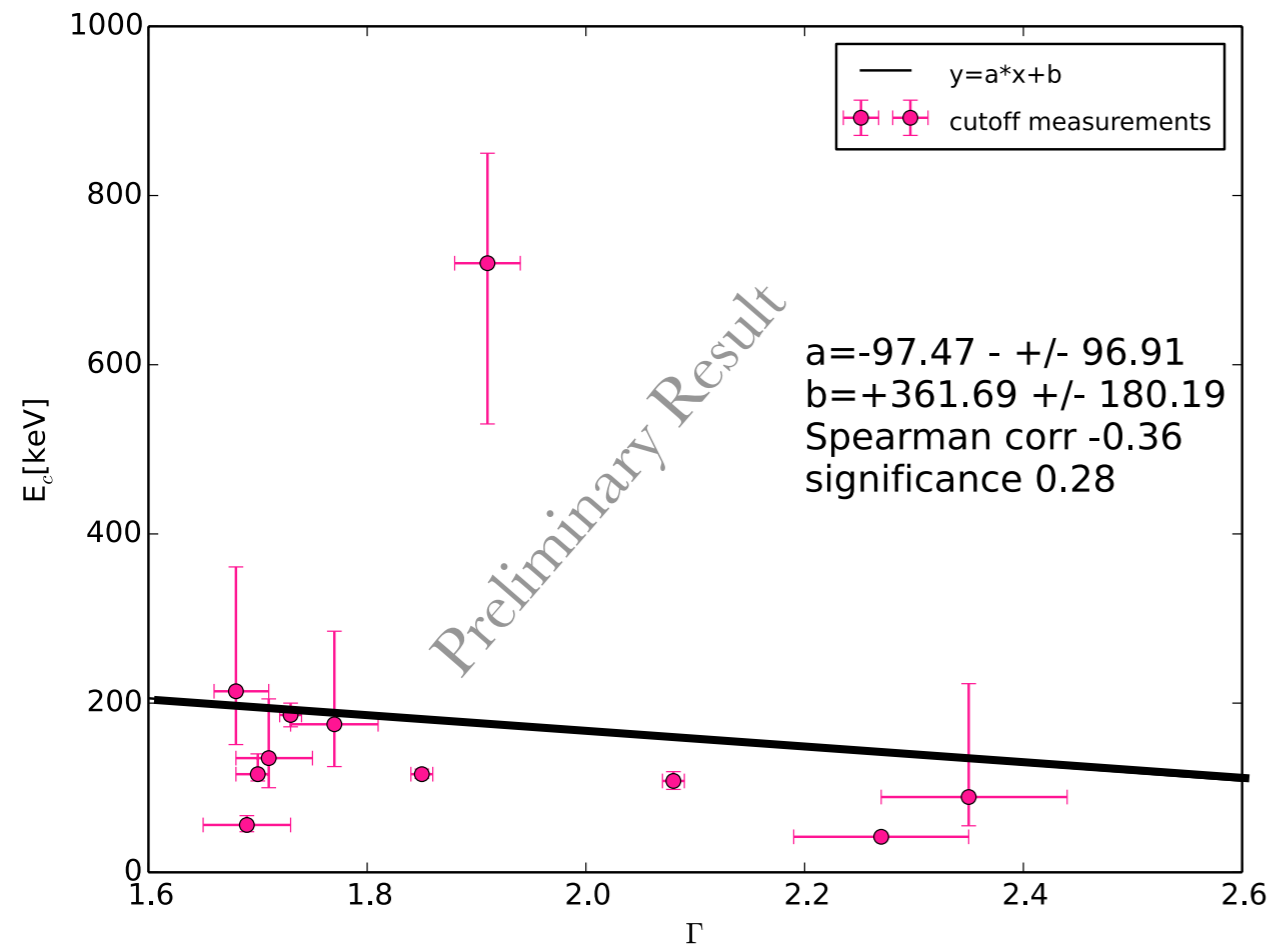
Eddington ratio



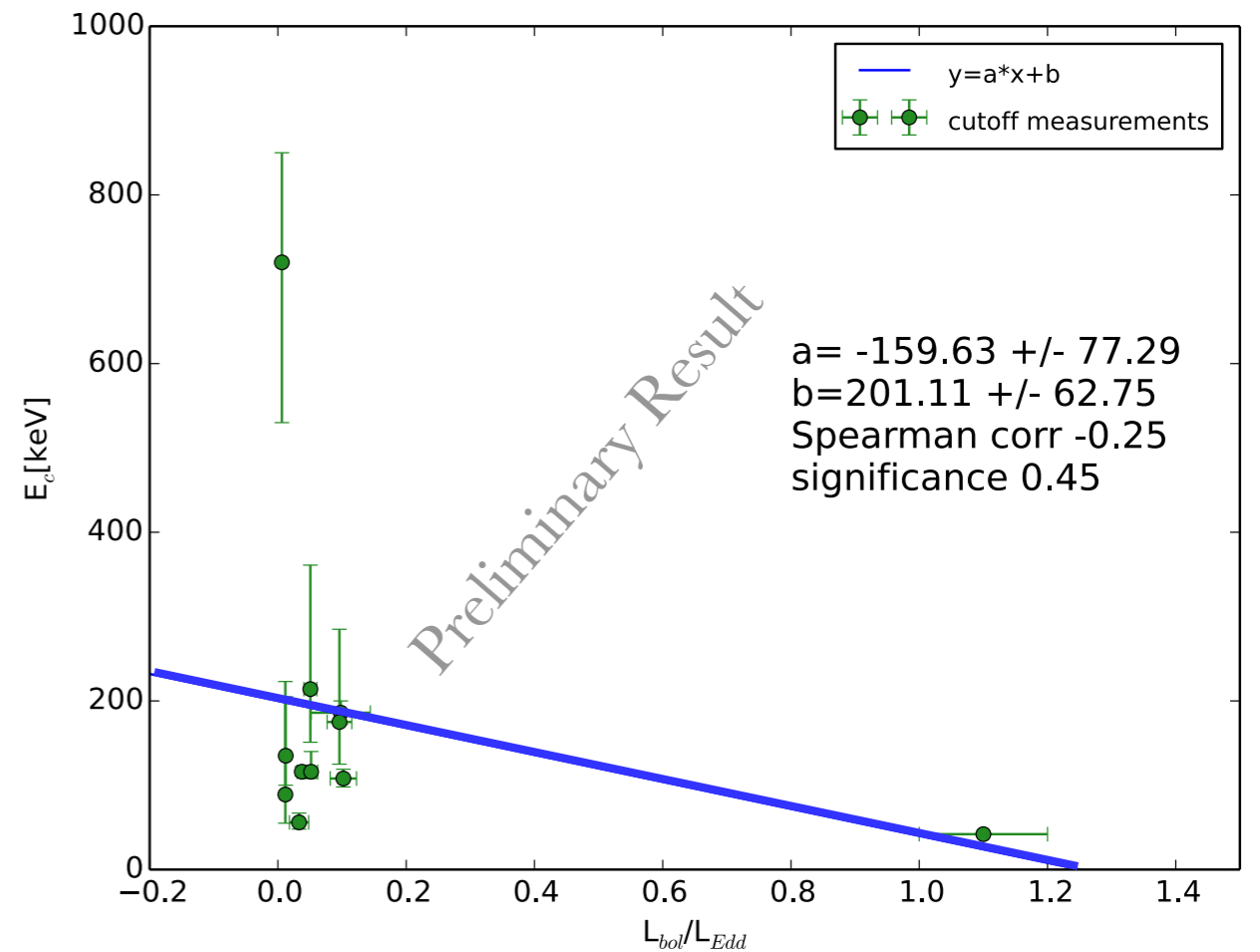
Looking for correlations

Fitting only the sources with cutoff measurements, with a simple linear relation:

Photon Index



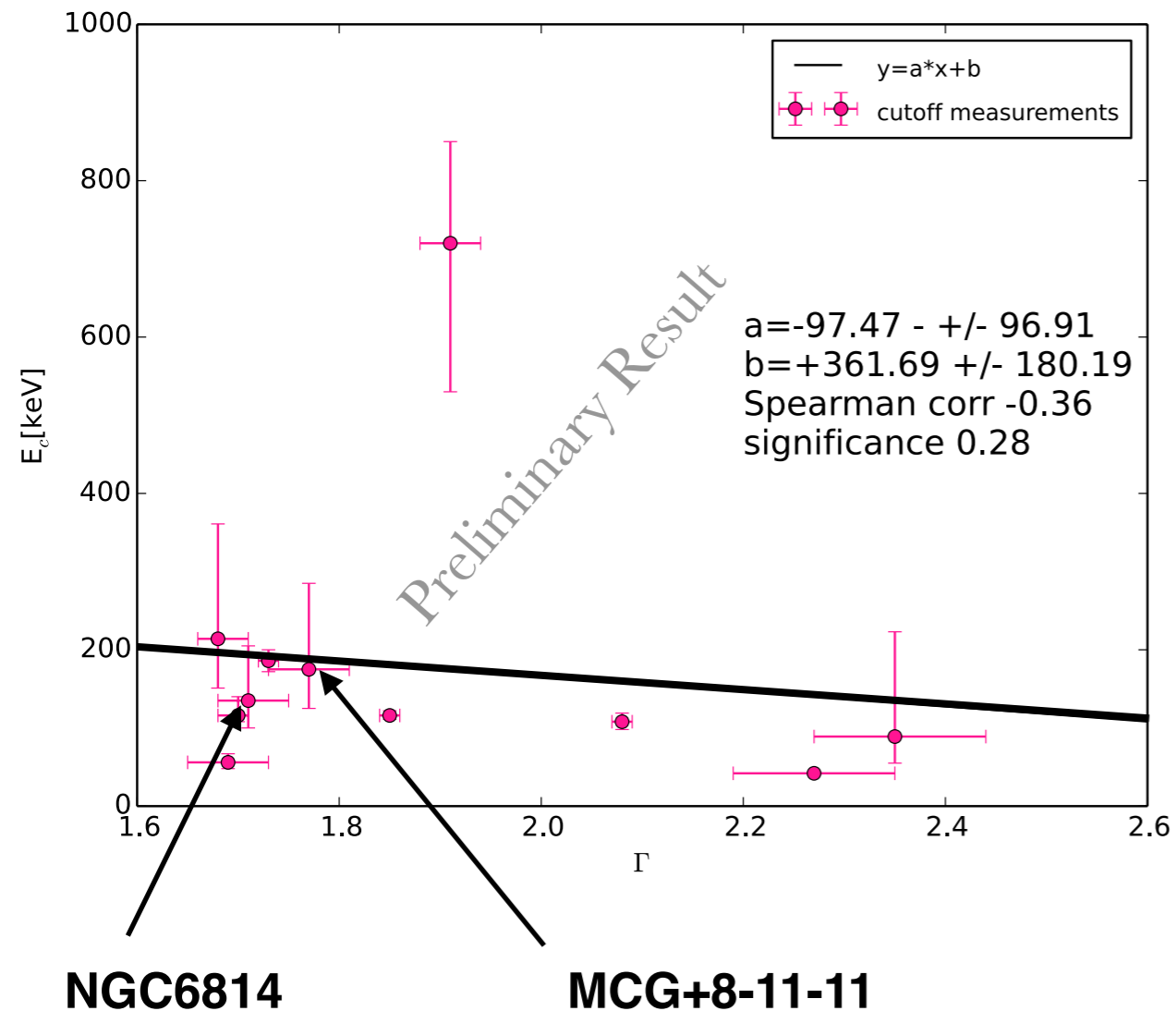
Eddington ratio



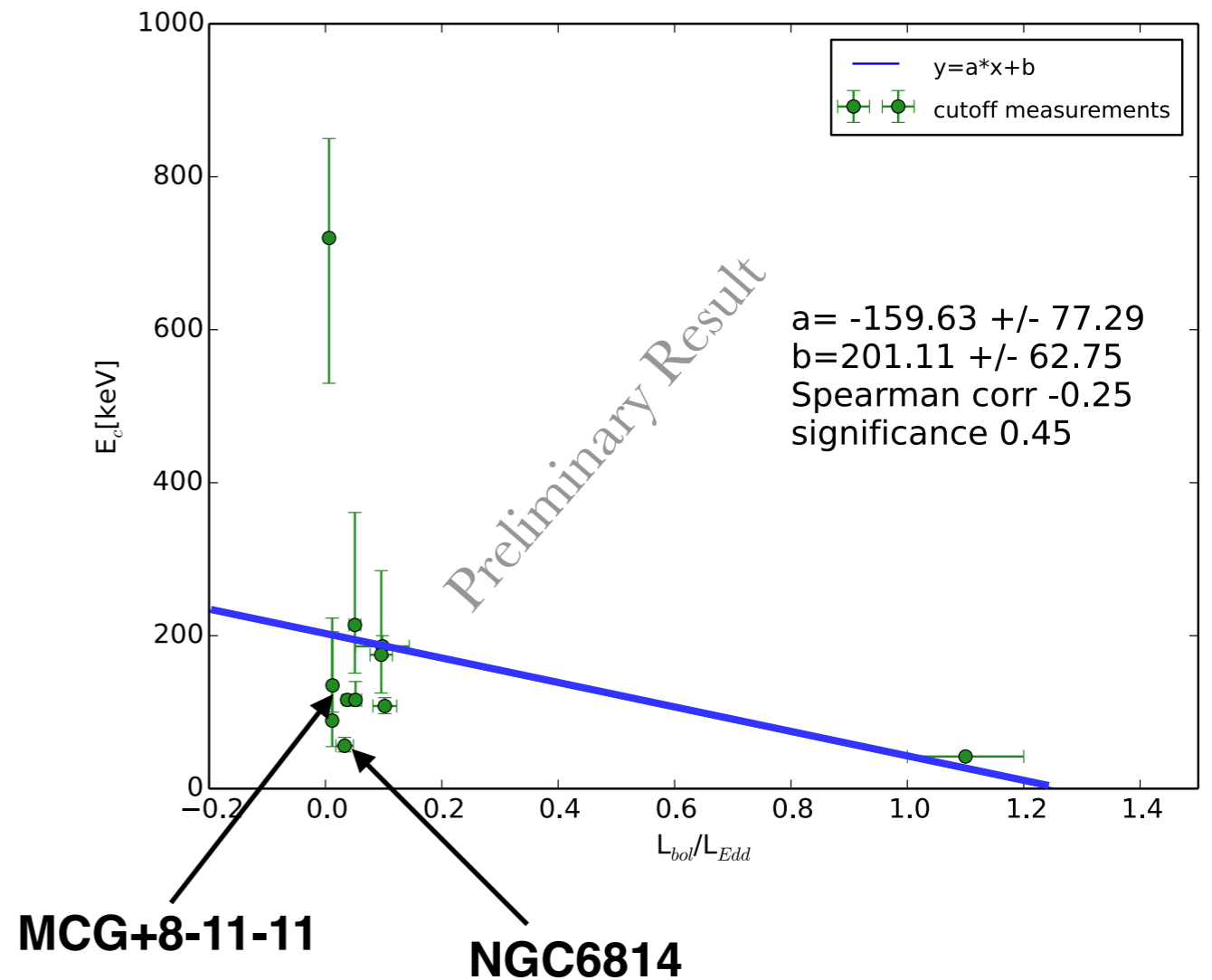
Looking for correlations

Fitting only the sources with cutoff measurements, with a simple linear relation:


Photon Index



Eddington ratio



Conclusion

- Cutoff measurements;
 - Relativistic broadened FeK α line with disk reflection component;
 - Narrow FeK α line due to a large iron overabundance, or alternatively produced in distant Compton thin material;
 - Estimated Eddington ratio $\eta=0.01$ for MCG +8-11-11 and $\eta=0.09$ for NGC 6814;
 - Both sources are located against the pair runaway line like most of the sources among those analyzed by Fabian et al.;
 - The observation of the two sources could help to understand the physics of the corona-accretion disk system and its geometry, enriching our sample;
-  Next step: fitting with the cutoff lower limits.



THANK YOU!